Gulf Stream Fluctuations and Meanders over the Onslow Bay Upper Continental Slope

DAVID A. BROOKS AND JOHN M. BANE, JR.[1]

Texas A&M University, College Station, TX 77843

(Manuscript received 9 June 1980, in final form 4 November 1980)

ABSTRACT

Gulf Stream fluctuations observed over the 200 and 400 m isobaths off Onslow Bay, North Carolina have a prominent weekly time scale. The principal fluctuations observed during the 4-month winter experiment are consistent with Webster's (1961a) description of downstream propagating, skewed, lateral meanders of the Gulf Stream over the upper continental slope. The subtidal velocity fluctuations were highly coherent over the vertical extent (~120 m) and over the horizontal extent (64 km) of our array. The implied downstream propagation speed was ~30 km day^{-1} for the weekly period meanders. Concurrent satellite images of a sea surface temperature (SST) meander pattern indicate that subsurface temperature, salinity, velocity and relative-vorticity maxima occurred as meander crests (shoreward SST-front excursions) passed over the experiment site. The meandering currents were not coherent with nearby wind stress or coastal sea level fluctuations. Eddy-flux estimates indicate energy conversion from the fluctuations to the mean Stream.

1. Introduction

Gulf Stream eddies and inshore countercurrents have a written history of almost four centuries. Considering that the Gulf Stream itself was first noted by Ponce de Leon in 1513, it is remarkable that only a few decades later John White (1590, p. 608), in a logbook account of his second Roanoke voyage, gives a detailed description of the "eddie currents setting to the south and southwest" along the Carolina coasts. White's narrative style suggests that he was merely recounting common knowledge. It is likely that a working knowledge of Gulf Stream eddies in this area was available in the mid-sixteenth century, since the efficacy of the Gulf Stream return route to Europe had been well established by that time.

Webster (1961a) studied the near-surface velocity and temperature structure of Gulf Stream meanders and their associated inshore eddies off Onslow Bay, North Carolina. His study was based on GEK and bathythermograph data from 120 consecutive crossings of the Stream in a 28-day period. He characterized the meanders as skewed, wavelike, lateral oscillations in the offshore position of the Gulf Stream front, with dominant fluctuation time scales of about 1 week and 4 days. Richardson *et al.* (1969) made 10 dropsonde transects of the Stream in the same area between June and July 1968, giving a 2-month mean velocity section, but with insufficient time resolution to study the meander details.

In 1976, we proposed an experiment to study the subsurface currents over the upper continental slope off Onslow Bay. In this paper, we present a preliminary description of the fluctuating fields during a 4-month winter mooring period, a calculation of their eddy exchange with the mean Gulf Stream, and a case study of the fluctuations that occurred as a satellite-observed sea surface temperature (SST) meander pattern passed through the experiment area.

2. Experiment description and basic statistics

Four subsurface, taut-wire moorings were deployed in an L-shaped array aligned with the continental-slope topography off Onslow Bay, North Carolina (Fig. 1). The moorings were similar to those described by Lee and Schutts (1977), each supporting several Aanderaa current, temperature and conductivity recording instruments in the lower half of the water column from 16 January to 14 May 1979. The nominal array design placed mooring A on the 200 m isobath with instruments at depths of 100 and 180 m, and moorings B, C and D on the 400 m isobath with instruments at depths of 260, 320 and 380 m (320 m excluded at B). The actual depths are shown in Table 1.

The sampling interval was 20 min for all instruments. The raw current and temperature time series were low-pass filtered with a 3 h quarter-power-period Lanczos filter kernel to reduce sampling noise. The resulting 3 HRLP time series were then split by a Lanczos 40 h filter into low-passed (40 HRLP) and bandpassed (3–40 HRBP) time series for further

[1] Present affiliation: Curriculum in Marine Sciences and Department of Physics, University of North Carolina, Chapel Hill, NC 27514.

0022-3670/81/020247-10$06.50

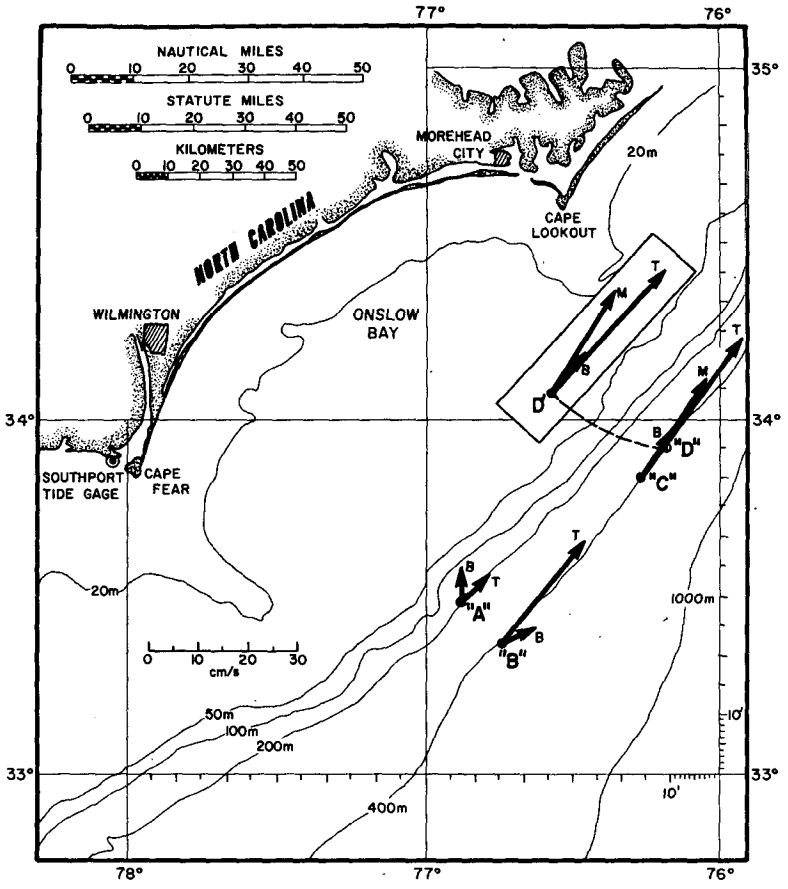

FIG. 1. Map of experiment area, showing locations of moorings A, B, C and D. The record-long mean current vectors are shown at each mooring for the top (T), middle (M) and bottom (B) instruments (see Table 1 for instrument depths). The current vectors at mooring D are shown displaced for clarity (inset box).

analysis.[2] The 40 HRLP data set contains fluctuations with periods > 40 h; tidal, inertial, and shorter periods are confined to the 3–40 HRBP data set. The bulk of the discussion here concerns the 40 HRLP data. The coordinate frame for all data has been rotated 34° clockwise to align with the local topography, such that the (u, v) velocity component is positive in the (offshore, downstream) direction.

Basic statistics of the current-velocity component and temperature time series are shown in Table 1. The variance ratios in Table 1 show that the tidal and shorter period motions accounted for typically only 10% of the total 3 HRLP temperature and v-component variance, whereas they accounted for typically 30% of the u-component total, with larger fractions occurring inshore and near bottom. The downstream-velocity-component fluctuations typically had standard deviations several times their means. The mean 3 HRLP velocity vectors for the entire record are shown in Fig. 1. The largest departure from the downstream direction occurred at the deepest instrument on the A mooring (A-bot), where the mean vector had an onshore component, the v component had its smallest mean, and the semidiurnal tidal motions were relatively strong.

3. Gulf Stream fluctuations

Current, temperature and salinity (conductivity) records from instrument A-top are shown in Fig. 2 for the first 30 days of the mooring period. The current velocity is characterized by approximately weekly time-scale fluctuations in magnitude and sign. During the first 30 days, the downstream (v) component extrema were 110 and -60 cm s^{-1}, occurring at times of maximum semi-diurnal tidal modulation. In the subtidal records, the offshore (u) component maxima, typically 20 cm s^{-1}, led the v component maxima, typically 75 cm s^{-1}, by less than one day. Temperature and salinity maxima occurred nearly simultaneously and less than one day after v compo-

[2] 3 HRLP means "3 hour low-pass" filtered and 3–40 HRBP means "3–40 hour band-pass" filtered, where the hours specified define quarter-power (−6 dB) periods of the filter energy response.

TABLE 1. Minimum, maximum, mean, standard deviation and variance ratios for temperature (T, °C), offshore velocity component (u, cm s^{-1}), and longshore velocity component (v, cm s^{-1}). The water depth/instrument depth (m) is shown after each instrument name.

Instrument	Variable	Minimum	Maximum	Mean	Standard deviation	Variance ratios	
		3 HRLP				3–40 HRBP/3 HRLP	40 HRLP/3 HRLP
A-top (198/98)	T	12.5	23.8	17.2	1.8	0.09	0.91
	u	−38.6	48.8	0.2	9.8	0.56	0.44
	v	−70.6	116.8	7.0	33.9	0.06	0.91
A-bot (198/178)	T	3.9	19.5	11.5	3.3	0.11	0.83
	u	−31.5	44.4	−2.7	9.1	0.66	0.30
	v	−58.5	74.7	4.0	21.0	0.10	0.84
B-top (390/250)	T	8.8	18.7	12.6	2.5	0.03	1.00
	u	−55.6	63.8	1.3	15.7	0.18	0.81
	v	−49.5	134.0	25.1	29.3	0.06	0.94
B-bot (390/370)	T	6.2	14.4	8.9	1.5	0.04	0.87
	u	−33.6	39.5	2.3	11.0	0.33	0.64
	v	−62.6	53.4	4.7	17.3	0.09	0.88
C-top (385/245)	T	9.2	18.1	12.8	2.1	0.06	0.95
	u	−33.2	54.3	4.3	11.5	0.31	0.67
	v	−44.0	135.1	32.3	33.6	0.05	0.95
C-mid (385/305)	T	3.2	29.5	11.2	1.8	0.09	0.81
	u	−98.8	83.2	−0.2	16.1	0.18	0.67
	v	−45.7	112.6	22.9	26.6	0.07	0.96
C-bot (385/365)	T	7.2	14.4	9.4	1.1	0.25	0.83
	u	−33.4	48.0	−0.5	9.5	0.76	0.23
	v	−39.8	74.4	9.3	19.8	0.10	0.93
D-top (376/236)	T	8.5	18.8	13.2	2.0	0.10	0.90
	u	−28.1	48.2	4.0	10.2	0.37	0.66
	v	−34.9	121.6	31.5	28.7	0.06	0.98
D-mid (376/296)	T	7.6	19.0	11.3	1.7	0.10	0.90
	u	−29.5	41.9	−1.3	8.8	0.43	0.53
	v	−46.0	116.0	24.3	28.8	0.05	0.97
D-bot (376/356)	T	6.7	13.6	9.3	1.1	0.17	0.83
	u	−26.9	34.8	0.1	7.8	0.78	0.24
	v	−38.2	55.1	7.9	16.8	0.10	0.93

nent maxima. As shown in Table 1, tidal fluctuations accounted for almost half of the u component record-long variance at A-top, whereas they accounted for only ~10% of the v-component variance there.

During the first two weeks of February, we obtained eight quasi-synoptic, three-dimensional "views" of the thermal structure of the Gulf Stream frontal zone between Charleston, South Carolina, and Cape Hatteras, North Carolina. These data were obtained from aircraft-dropped expendable bathythermograph (AXBT) probes. A description of the horizontal temperature field structure at various depths and a comparison with the currents has been given by Bane *et al.* (1980) for the period including the 5 and 11 February v component maxima shown in Fig. 2. They found that the subsurface temperature fields had a downstream-moving, vertically coherent, skewed wavelike structure. The temperature field skewness reflected the subtidal v component skewness evident in Fig. 2 during February, with the in-phase AXBT temperature and velocity increases occurring during a longer time interval than did the decreases at the same location. Webster (1961a) noted a similar upper layer temperature field and surface velocity skewness in his Onslow Bay data, which he associated with the downstream passage of asymmetric lateral meanders in the Gulf Stream front, having a weekly time scale. In view of the similarities between Webster's observations and ours, we will refer to fluctuations having a prominent weekly time scale, such as those in Fig. 2, as meander-related, or just "meanders." This of course does not rule out other potentially important mechanisms for Gulf Stream fluctuations.

The v component subtidal current fluctuations have a prominent autospectrum peak at a 7–8 day period, as shown for representative instruments in Fig. 3a. Less prominent but distinct peaks also are

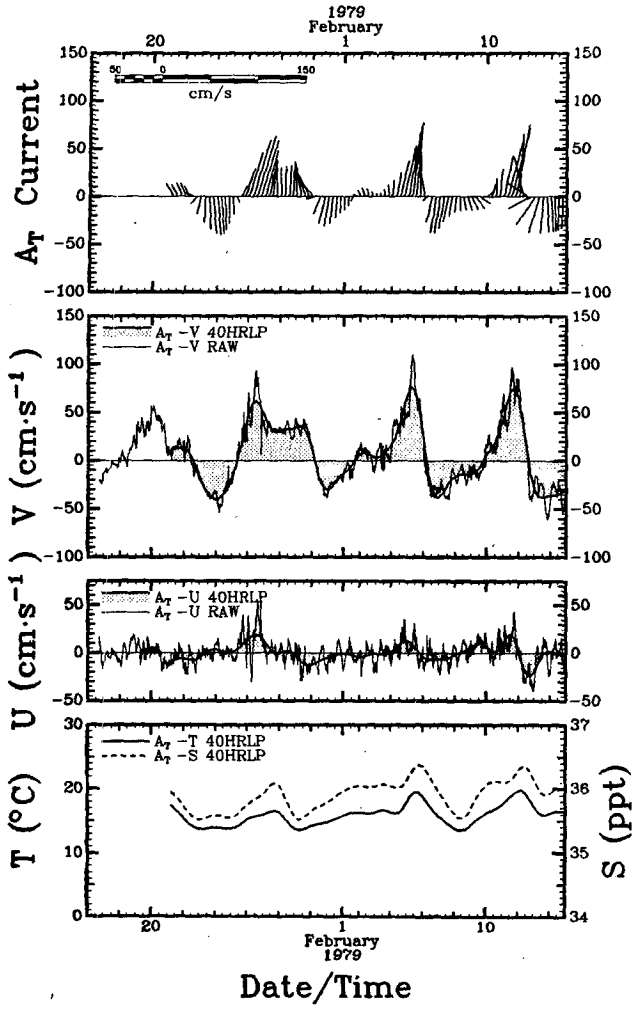

FIG. 2. Velocity vectors, velocity components (v, u), temperature (T) and salinity (S) from the top instrument on mooring A (A_T) for the first 30 days of the experiment. Vectors pointing "up" indicate flow in the downstream ($+v$) direction; the offshore ($+u$) direction is 90° clockwise therefrom. The "raw" data (thin lines) are unfiltered, and the "40 HRLP" data (heavy and dashed lines, and vectors) have been 40 h low-pass filtered to remove tidal and inertial fluctuations. Times are Greenwich Mean Time (GMT).

apparent at 3.3- and 2.5-day periods in the B and C mooring records, but they are suppressed at A-top. The u components (not shown) generally display similar prominent but smaller amplitude autospectrum peaks. For comparison, it is useful to normalize the peak spectrum densities for each instrument (Fig. 3a) by the square of the subtidal mean v component for that instrument. The result, when multiplied by the spectrum bandwidth, is an estimate of the fluctuation-to-mean downstream kinetic energy ratio in a 0.033 cpd frequency band centered on the peak frequency. For the 7–8 day period peaks, the ratios are 6.8, 0.23, 3.3 and 0.26 for instruments A-top, B-top, B-bot and C-top, respectively. For 15 degrees of freedom of the spectrum estimates in Fig. 3, the upper (lower) 95% confidence limit on each energy ratio is ~1.6 (0.6) times its value. In this band, the fluctuation kinetic energy is considerably larger than the mean at the inshore and near-bottom instruments, but it is only about one-fourth the mean value at the mid-depth instruments and remains statistically invariant over the 64 km separating the B and C moorings.

The current fluctuations in the 2–10 day period band were highly coherent over the 64 km separating the B-top and C-top instruments (Fig. 3c). The peaks in the coherence between the v components at B-top and C-top generally coincide with those in the cross spectrum (Fig. 3b), indicating selective organization of the fluctuations over the scale of the array for the

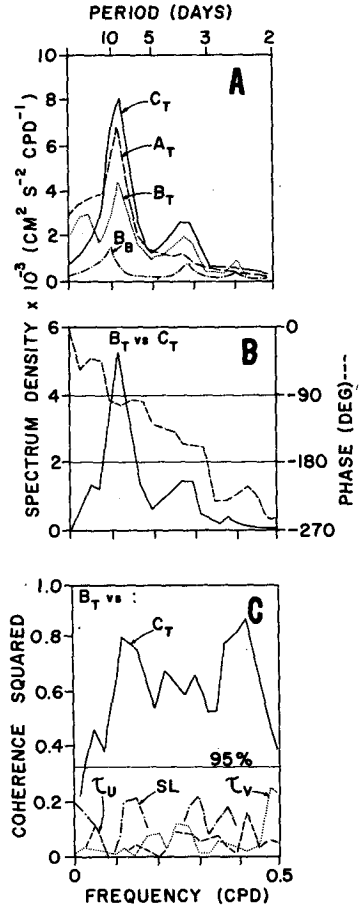

FIG. 3. Spectrum density for the v component velocity fluctuations at selected instruments (A); cross-spectrum density and phase between v component fluctuations at instruments B-top and C-top (B); coherence squared between the B-top v component (B_T) and the C-top v component C_T, the offshore wind stress τ_u, the longshore wind stress τ_v and coastal adjusted sea level fluctuations SL (C). Negative phase means C-top lags B-top. The 95% significance level is shown for coherence squared. The spectrum estimates were computed with 15 degrees of freedom, and the effective bandwidth is 0.033 cycles per day (cpd).

periods noted. Over the coherent frequency range, the C-top fluctuations lag those at B-top. The approximately linear relation between phase and frequency for the v components (Fig. 3b) indicates an average downstream propagation speed of 48 km day^{-1} for fluctuations of period 2–10 days. In the 7–8 day period band, the approximately 100° phase lag indicates a wavelength of 230 km, corresponding to downstream propagation speeds of 33 to 29 km day^{-1}.

The periods of the autospectrum peaks shown in Fig. 3a are similar to those noted by Webster (1961a). He reported 6.9-, 3.9- and 2.7-day period oscillations of the lateral position of the 100 m depth of the 20°C isotherm, chosen because it coincided with the path of maximum downstream surface velocity. The shorter period spectrum peaks and their relative amplitudes may give useful information about harmonic distortion of the meandering process. Webster also noted a possibly "coincidental" correlation between the offshore position of the downstream surface velocity maximum and the offshore wind component (inferred from longshore pressure differences). We have found no significant subtidal correlation between the B-top v component and either wind stress component at an offshore meteorological buoy located on the 100 m isobath ~200 km upstream of mooring B (Fig. 3c). Similar calculations for the current-velocity components at other instruments and also for Cape Hatteras wind data consistently indicate near-independence of the subtidal-current and wind-stress fields (Brooks *et al.*, 1980).

A coherence structure similar to that between the B-top and C-top v components (Fig. 3c) has been noted between North Carolina coastal sea level records (Brooks, 1978). The similarity suggests a frequency-selective coupling between coastal sea level and offshore current fluctuations. The coherence between the B-top v component and barometrically adjusted Southport sea level (Fig. 3c), however, shows only hints of peaks near the prominent periods mentioned. None of the peaks reaches values statistically significant at the 95% level. Slightly higher coherences were found for certain combinations of current components and coastal sea level records from several tide gages (not shown), but we conclude that the current fluctuations over the continental slope off Onslow Bay and coastal sea level fluctuations were at most very weakly coupled during our experiment.

4. Relationships between a SST meander and subsurface fluctuation fields

Between 27 and 29 March, the B-top v component increased by almost an order of magnitude (Fig. 4). This was accompanied by a less rapid increase in offshore flow, which reached a maximum ~¼ day before the v component maximum. Large temperature and salinity increases (~8°C, 1.4‰) occurred almost simultaneously with the v component increase.

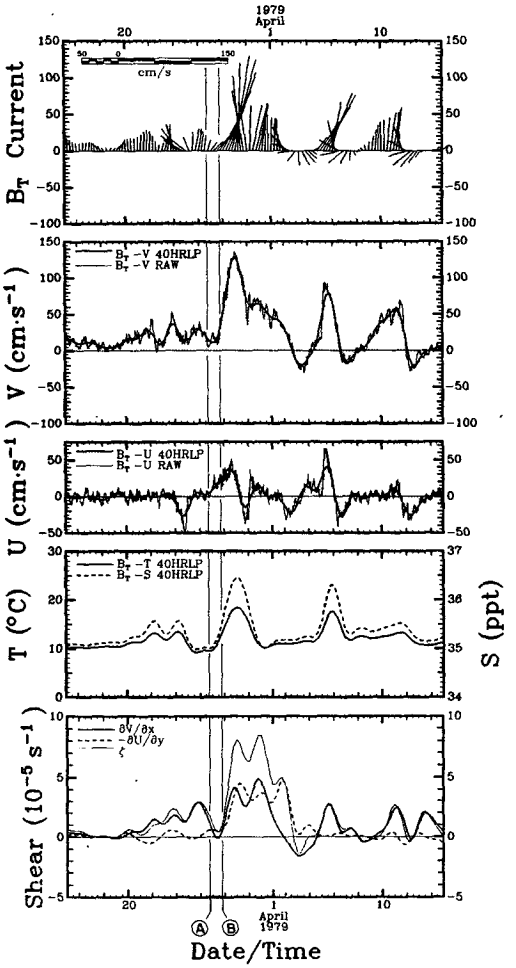

FIG. 4. As in Fig. 2 except for the period 15 March–15 April 1979, and showing the 40-HRLP relative vorticity (ζ) and its components (bottom panel). The $-\partial u/\partial y$ component has an artificial lead of 36.5 h (see text). The times identified by the vertical lines labeled A and B are the times of the satellite SST images shown in Fig. 5a and 5b, respectively.

Satellite SST images taken at the times shown by the vertical lines in Fig. 4 show a pronounced wavelike meander pattern in the Gulf Stream off the Carolina Capes (Fig. 5). Large-amplitude SST meanders are often found in this area and are thought to be wake phenomena associated with a topograph irregularity on the outer continental shelf off Charleston, South Carolina (Legeckis, 1979). Smaller scale meanders also occur upstream of Charleston (Lee *et al.*, 1980; Lee and Brooks, 1979). A SST meander crest[3] was approaching the B mooring position at

[3] We define a satellite SST meander crest to be the local shorewardmost excursion of the surface temperature front defining the boundary between Gulf Stream and shelf water; the local seawardmost excursion of the front will be called a "trough."

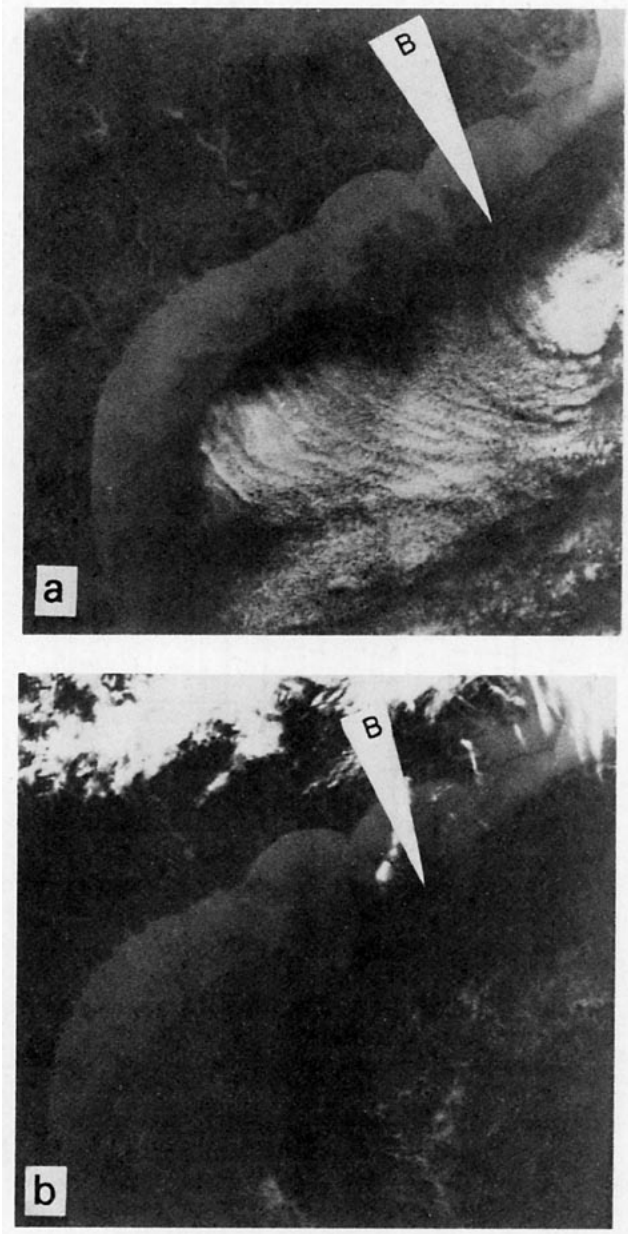

FIG. 5. Gray-scale rendition of satellite SST infrared images, showing a wavelike Gulf Stream meander structure off the Carolina bays at 1957 GMT 26 March (a) and 1947 GMT 27 March 1979 (b). Local times were 5 h earlier (mid-afternoon). Darker shades of gray indicate warmer Gulf Stream waters. White areas are clouds; the meander pattern in (a) is repeated in the cloud structure. The central crest of the meander pattern was about to pass over the mooring-B location, shown approximately by the arrowhead. A warm "filament" on the inshore edge of the Stream extends from off Cape Hatteras (the upper rightmost cape) southwestward toward mooring B.

the times of the images in Fig. 5. The rapid increase in the B-top v component was just beginning at the time of the second image (Fig. 5b). It is apparent that the subsequent passage of the SST meander crest over the mooring was closely associated with the v component maximum in Fig. 4, which occurred about one day later than the image in Fig. 5b. The SST image from that day was partially obscured by clouds and is not shown.

An elongated warm filament, separated from the main Stream by a tongue of relatively cool water, can be seen in the SST images (Fig. 5). The filament extended from Cape Hatteras upstream into Onslow Bay. The thermal structure of a similar warm filament transected by our AXBT survey was confined to the top few tens of meters, but the cool water between it and the main Stream extended to a depth of at least 400 m (Bane *et al.*, 1980). The uplifting of isotherms which defines the cool tongue of water in a meander trough suggests that upwelling is associated with the meandering process, but it is not presently clear whether the upwelling occurs locally or upstream. Atkinson *et al.* (1980) showed that intrusions of deep, cold Gulf Stream water into Onslow Bay are associated with Gulf Stream motions. Observations made upstream of our study area (Lasley *et al.*, 1979; Lee and Brooks, 1979; Lee *et al.*, 1980) have shown that shoreward eddies along the Gulf Stream front often contain a cold core of water with temperature, salinity and nutrient properties indicative of upwelling. Thus the upwelling may be initiated upstream of Onslow Bay, although the evolution of a meander during its northeastward propagation probably requires the upwelling process to evolve as well.

Figs. 2, 4 and 6 show that our current meters at moorings A and B often sensed cyclonic velocity vector rotation and countercurrents as meander crests passed by. The fate of the southwestward moving water is unclear from our data. The satellite SST images in Fig. 4 and in other sources (Legeckis, 1979) do not show warm filaments reentering the Stream to form closed-off cyclonic vortices, although occasionally filaments turn seaward southwest of cool tongues and partially envelop them (e.g., Brooks *et al.*, 1980). Part of the southwestward moving water may be returned to the north within the shoreward side of the warm filament, in association with the isotherms defining that part of the filament (e.g., Bane *et al.*, 1980). Pietrafesa and Janowitz (1979) noted that the shallow (<50 m) current vectors over the shelf off Charleston rotated anticyclonically as the shoreward "edge" of a Gulf Stream filament passed over their mooring.

From our data set, we can estimate the vertical relative vorticity (ζ) components $\partial v/\partial x$ and $-\partial u/\partial y$. The subtidal estimates were computed as $\partial v/\partial x = (v_{\text{B-top}} - v_{\text{A-bot}})\Delta x^{-1}$ and $-\partial u/\partial y = (u_{\text{C-mid}} - u_{\text{D-mid}})\Delta y^{-1}$, where $(\Delta x, \Delta y) = (18, 12)$ km. The mid-depth instruments were used for $-\partial u/\partial y$ because D-top failed on 22 March. The $-\partial u/\partial y$ component was given a lead of 36.5 h to allow for the mean propagation time between the B mooring and the midpoint of the C and D moorings. One possible

source of error in the $\partial v/\partial x$ calculation is the 72 m depth difference between the B-top and A-bot instruments.

The relative vorticity components and their sum are shown in Fig. 4 for 15 March–15 April. Relative vorticity maxima occurred almost simultaneously with v component maxima. The SST meander of Fig. 5 was accompanied by a positive vorticity peak of 8×10^{-5} s^{-1}, occurring less than one day after the v component maximum. For comparison, the local vertical value of the planetary vorticity (Coriolis parameter) is 8.2×10^{-5} s^{-1}. Smaller vorticity peaks are associated with the meanders of 5 and 11 April in Fig. 4. Relative vorticity maxima, occurring near or slightly upstream of meander crests, appear to be a characteristic feature of meanders.

The velocity fluctuations associated with the passage of the meander crest discussed above and with later meanders exhibit a high degree of vertical and horizontal visual coherence (Fig. 6). In this figure, the C-top vectors are shown with a time lead of 33 h, which gives maximum correlation between the B-top and C-top v components over the 4-month record length. The 33 h phase difference corresponds to an average downstream fluctuation propagation speed of 46.5 km day^{-1} over the 64 km distance between moorings B and C, consistent with the phase calculations of Section 3. The alignment in Fig. 6 emphasizes the similarities between the flow features at C-top and the other instruments, including the arrival at mooring C of the meander crest discussed above. Differences in detail are also apparent. For example, fewer current reversals occur at C-top than at B-top, but this may reflect the stronger mid-depth mean flow at the downstream mooring (Table 1 and Fig. 1), rather than evolution of the meandering process. The kinetic energy ratios discussed in Section 3 do not indicate a significant downstream change of relative intensity in the weekly meandering. The northeastern crest of the meander pattern in Fig. 5 evidently caused only weak velocity fluctuations at the B mooring, but it may be associated with a prominent C-top velocity fluctuation (Fig. 6). In some cases, for example, on 3 and 12 April, the southwestward flow at the B mooring appears to be bottom-intensified, which may indicate the importance of topographic effects as the Stream abuts against the continental slope.

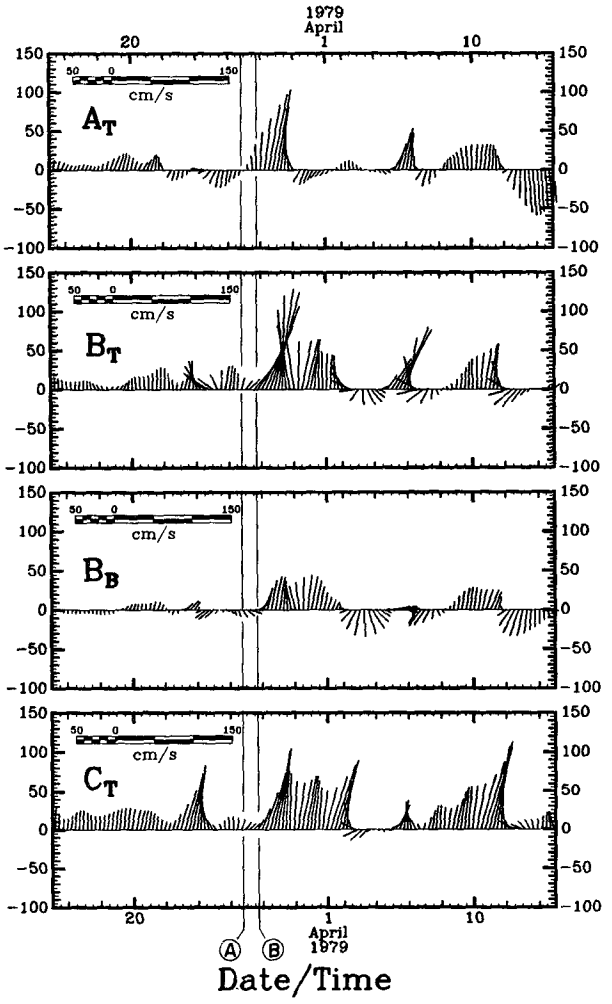

FIG. 6. Current vectors showing subtidal (40 HRLP) fluctuations at the A, B and C moorings. Mid-depth ("top") instruments have T subscripts, near-bottom instruments have B subscripts. The vector sense is the same as for Fig. 2. The C_T vectors have an artificial lead of 33 h, which accounts for the mean downstream fluctuation propagation time and emphasizes the similarities in the records. The vertical lines A and B mark the times of the SST images in Figs. 5a and 5b, respectively.

5. Eddy energy transfer

Lee and Mayer (1977) inferred that spin-off eddies emerged as barotropic instabilities of the Florida Current. This implies Reynolds-stress kinetic-energy conversion from the mean to the fluctuating motion. Webster (1961b) concluded from GEK observations that the energy conversion favored growth of the fluctuations along the extreme western edge of the Florida Current, but that the net (cross-Stream integrated) energy transfer was to the mean Current. Using a free-fall instrument data set, Schmitz and Niiler (1969) confirmed Webster's results in the cyclonic zone of the mean Florida Current, but they found no evidence of net energy transfer between the mean current and the fluctuations. They concluded instead that internal redistribution of kinetic energy could explain the observations with no need for an external energy source.

From GEK observations in the Onslow Bay area, Webster (1961b) found that net energy was transferred from meanders to the mean Stream at a rate sufficient to double the mean surface kinetic energy in 11 days, which is less than two meander periods.

This surprising "negative eddy viscosity" placed the energy source of the meanders in doubt, since Webster also showed that the kinetic energy contributed to meanders by the wind stress is at least an order of magnitude smaller than that transferred from the meanders to the mean Stream.

Following Webster (1961b) and Schmitz and Niiler (1969), we assume here that the most significant term in the net eddy-kinetic-energy transfer from the fluctuations to the mean Stream is $\rho\overline{u'v'}\partial\bar{v}/\partial x$. The overbar average is a time mean taken over the length of the time series, or a portion of it, and primes denote departures from the mean. The x values increase in the offshore direction, and we set the density $\rho = 1\ \mathrm{g\,cm^{-3}}$. A number of potentially important terms have been excluded from consideration (e.g., Webster, 1961b). Because our data set does not span the entire Stream, calculation of $\rho\overline{u'v'}\partial\bar{v}/\partial x$ from cross-stream pairs of current meters gives only the contribution to the net energy transfer and not necessarily the total local conversion rate for the pair.

Estimates of the momentum flux term $\overline{u'v'}$ and the net rate of kinetic-energy transfer from the fluctuations to the mean Stream, calculated from our subtidal current records at moorings A and B, are shown in Table 2. The averaging was done over the full 110-day record length and also over a 7-day period including the meander discussed in Section 4. The mean shear for the "top" (mid-depth) instruments was calculated as $(\bar{v}_{\mathrm{B-top}} - \bar{v}_{\mathrm{A-top}})/\Delta x$ where $\Delta x = 18$ km, and similarly for the near-bottom instruments.

The energy flux estimates shown in Table 2 indicate a mid-depth contribution to net eddy conversion of energy from the fluctuations to the mean Stream off Onslow Bay, consistent with Webster's (1961b) estimates for the surface layer. The near-bottom estimates are essentially zero, because the mean shear was very small there. The mid-depth estimates are about a factor of 4 smaller than Webster's, possibly because the relatively wide spacing of our moorings underestimated the mean shear. During the meander period, the mid-depth conversion rate increased to more than twice that of the full-record rate, with worst-cast error limits considered, indicating the importance of meander events in the conversion process. The momentum fluxes were divergent at mid-depth and near-bottom, also consistent with Webster's results in the cyclonic zone, indicating retardation of the inshore edge of the mean Stream. The momentum flux was offshore at all instruments except A-bot, where the mean Stream also had a relatively strong onshore component.

The offshore eddy energy flux values in Table 2 result from positive correlations of the fluctuation velocity components in the presence of cyclonic horizontal shear of the mean Stream. Positive $\overline{u'v'}$ correlations imply that the fluctuation streamlines are skewed (elliptical) with a positive average semi-major axis slope (Pedlosky, 1979, p. 435). Thus the offshore energy fluxes reported here and by Webster (1961b) are consistent with the positive skewness sense discussed in Section 3. The same skewness sense was apparent in the subsurface thermal field during part of this experiment (Bane *et al.*, 1980).

Oort (1964) calculated the surface-layer eddy heat flux from Webster's (1961a) Onslow Bay data set. He found an offshore heat flux, inconsistent with baroclinic conversion of mean potential energy to eddy energy in the top 200 m. The mid-depth and near-bottom eddy fluxes of temperature $\overline{u'T'}$ calculated from our data set, were also offshore or insignificant at the A and B moorings (Table 2), and are thus inconsistent with a baroclinic fluctuation energy source in the deeper layers. The largest temperature-flux values ($\sim$10 cm °C $\mathrm{s^{-1}}$) occurred at the B-top instrument, and were similar in magnitude to Oort's (1964) maximum value. The three-fold increase in $\overline{u'T'}$ at B-top during the meander-averaging period is not significantly different from the record-long average. The only other significantly

TABLE 2. Eddy energy and temperature fluxes calculated for the full 110 day record (F) and for the 7-day meander period 27 March–2 April (M), plus or minus one standard error. Positive flux values indicate offshore transport.

Instrument	Averaging time	$\bar{u}$ (cm $\mathrm{s^{-1}}$)	$\bar{v}$ (cm $\mathrm{s^{-1}}$)	$\hat{T}$ (°C)	$\overline{u'v'}$ ($\mathrm{cm^2\ s^{-2}}$)	$(\partial\bar{v}/\partial x) \times 10^{-5}$ ($\mathrm{s^{-1}}$)	$\rho\overline{u'v'}(\partial\bar{v}/\partial x) \times 10^{-5}$ (ergs $\mathrm{cm^{-3}\ s^{-1}}$)	$\overline{u'T'}$ (cm °C $\mathrm{s^{-1}}$)
A-top	F	0.13 ± 0.31	5.59 ± 1.55	17.1 ± 0.08	75.3 ± 13.5	1.05	79.1 ± 14.2	0.61 ± 0.65
	M	−0.74 ± 1.56	23.2 ± 7.31	17.5 ± 0.28	268 ± 80.6	1.87	501 ± 151	1.94 ± 1.94
B-top	F	1.29 ± 0.67	24.4 ± 1.36	12.6 ± 0.12	119 ± 23.1	1.05	125 ± 24.3	6.44 ± 1.57
	M	5.48 ± 3.26	56.8 ± 6.74	12.9 ± 0.57	263 ± 129	1.87	492 ± 241	17.5 ± 9.93
A-bot	F	−2.56 ± 0.24	2.94 ± 0.92	11.6 ± 0.14	−26.0 ± 6.12	0.05	−1.30 ± 0.31	4.18 ± 0.69
	M	−8.46 ± 0.75	20.9 ± 4.43	9.97 ± 0.57	−61.1 ± 10.2	−0.08	4.89 ± 0.82	0.16 ± 1.55
B-bot	F	2.24 ± 0.42	3.89 ± 0.78	8.95 ± 0.07	61.2 ± 8.14	0.05	3.06 ± 0.41	2.34 ± 0.46
	M	3.11 ± 1.45	19.5 ± 3.72	8.76 ± 0.31	38.8 ± 38.4	−0.08	−3.10 ± 3.07	−1.77 ± 1.68

non-zero values occurred at the near-bottom instruments for the full-record averaging period, with offshore fluxes of ~3 cm °C s^{-1}. Offshore eddy temperature flux is consistent with upwelling of cool water in a meander trough, as suggested in Section 4.

6. Concluding remarks

Meanders dominated the Gulf Stream fluctuation fields over the Onslow Bay upper continental slope during January to May, 1979. The mid-depth and near-bottom flow at current meters moored on the 200 and 400 m isobaths typically varied in magnitude with prominent weekly and 3–4 day time scales, similar to those noted by Webster (1961a). The offshore-flow-component maxima generally led the downstream-component maxima by less than one day as meanders passed by a fixed current-meter location. Temperature, salinity and relative-vorticity maxima occurred almost in phase with downstream-flow-component maxima. The velocity fluctuations were highly coherent and nearly in-phase vertically over the lower one-third to one-half of the water column; they were also horizontally coherent over the downstream scale (~64 km) of the array. The estimated mean downstream propagation speed was 46.5 km day^{-1} for the entire subtidal-fluctuation spectrum and ~30 km day^{-1} for meanders of period 7–8 days. We found no significant subtidal coherence between current and wind stress or current and barometrically adjusted coastal sea level fluctuations.

The principal subtidal fluctuations are consistent with Webster's (1961a) description of downstream-propagating, skewed, lateral meanders of the Gulf Stream. The case study in Section 4 suggests that temperature, salinity and velocity maxima occur as SST meander crests pass by and bring Gulf Stream water over a fixed observation point on the upper continental slope. Velocity vectors at our moorings rotated cyclonically as meander crests passed. Inshore countercurrents (southwestward flow) often occurred in meander troughs. Positive (cyclonic) relative vorticity peaks occurred near or slightly upstream of meander crests. That at times the countercurrents were bottom-intensified suggests the importance of topographic control as the Stream meanders over the slope. The fate of the upstream-moving water is not clear from our current observations, but supporting hydrographic data from Onslow Bay (e.g., Bane *et al.*, 1980) as well as earlier current observations in shallow (45 m) water upstream of Onslow Bay (Pietrafesa and Janowitz, 1979) suggest that part of it may be returned northeastward as a component of the shallow shelf circulation.

Eddy energy and temperature flux estimates from our data indicate a mid-depth net conversion of fluctuation to mean-Stream energy off Onslow Bay. The conversion rate was significantly larger during the meander case study of Section 4 than for the record-long case, indicating the importance of meanders in the conversion process. Near-bottom estimates were relatively small. Fluctuation-to-mean energy conversion in the cyclonic side of the mean Stream is consistent with the skewed meander features noted by Webster (1961a) and also apparent in our data set. Our mid-depth and near-bottom energy flux results extend some of Webster's (1961b) and Oort's (1964) upper layer results and imply upstream meander generation. The Stream deflection off Charleston, South Carolina and the subsequent rapid increase in SST meander amplitude upstream of Onslow Bay (Bane and Brooks, 1979; Legeckis, 1979) may be important elements in the energy budget of Gulf Stream meanders.

Acknowledgments. The Gulf Stream Meanders Experiment was supported by the National Science Foundation, under Grants OCE77-25682 and OCE 79-06710, and by the Office of Naval Research, under Contract N-00014-77-C-0354. The success of the field program was largely a result of the superb instrumentation and mooring talents of Mr. Paul Blankinship, aided by Messrs. Mitchell Malpass and David Leech. We acknowledge the essential efforts of oceanography graduate students at Texas A&M University, North Carolina State University and the University of North Carolina, who have devoted countless hours of work to this project on land and at sea. The satellite images were supplied by Dr. Richard Legeckis of NOAA/NESS, with whom we have had a longstanding and fruitful working relationship throughout all phases of this project. Most of the computer-graphics software was developed by Mr. Thomas Reid. We also extend our appreciation to Capt. Herbert Bennett and the crew of the R/V *Endeavor* for their effective services at sea. Professor Robert O. Reid, Dr. Worth D. Nowlin, Jr., and an anonymous reviewer provided helpful and clarifying suggestions for improvements of the manuscript.

DAB: I wish to record my respect and appreciation for the late Professor Walter Düing, who first showed me the power of the Gulf Stream.

REFERENCES

Atkinson, L. P., J. J. Singer and L. J. Pietrafesa, 1980: Volume of summer subsurface intrusions into Onslow Bay, North Carolina. *Deep-Sea Res.*, **27**, 421–434.

Bane, J. M., Jr., and D. A. Brooks, 1979: Gulf Stream meanders along the continental margin from the Florida Straits to Cape Hatteras. *Geophys. Res. Lett.*, **6**, 280–282.

——, —— and K. R. Lorenson, 1981: Synoptic observations of the three-dimensional structure, propagation and evolution of Gulf Stream meanders along the Carolina continental margin. *J. Geophys. Res.* (in press).

Brooks, D. A., 1978: Subtidal sea level fluctuations and their

relation to atmospheric forcing along the North Carolina coast. *J. Phys. Oceanogr.*, **8**, 481–493.

——, J. M. Bane, R. L. Cohen and P. Blankinship, 1980: The Gulf Stream Meanders Experiment. Current meter, atmospheric, and sea level data report for the January to May, 1979 mooring period. Ref. 80-7-T, Texas A&M University, 264 pp.

Lasley, S. R., L. P. Atkinson, J. J. Singer and W. S. Chandler, 1979: Hydrographic observations in the Georgia Bight (April, 1978). Tech. Rep. Ser. No. 79-5, University of Georgia, Skidaway Island, 94 pp.

Lee, T. N., and D. A. Brooks, 1979: Initial observations of current, temperature and coastal sea level response to atmospheric and Gulf Stream forcing on the Georgia Shelf. *Geophys. Res. Lett.*, **6**, 321–324.

——, and D. A. Mayer, 1977: Low frequency current variability and spin-off eddies along the shelf off southeast Florida. *J. Mar. Res.*, **4**, 193–220.

——, and R. L. Shutts, 1977: Technical program for Aanderaa current meter moorings on continental shelves. University of Miami, Tech. Rep. No. TR-77-5, 68 pp.

——, L. P. Atkinson and R. V. Legeckis, 1981: Detailed observations of a Gulf Stream spin-off eddy on the Georgia continental shelf, April 1977. *Deep-Sea Res.* (in press).

Legeckis, R. V., 1979: Satellite observations of the influence of bottom topography on the seaward deflection of the Gulf Stream off Charleston, South Carolina. *J. Phys. Oceanogr.*, **9**, 483–497.

Oort, A. H., 1964: Computations of the eddy heat and density transports across the Gulf Stream. *Tellus*, **16**, 55–63.

Pedlosky, J., 1979: *Geophysical Fluid Dynamics*. Springer-Verlag, 624 pp.

Pietrafesa, L. J., and G. S. Janowitz, 1979: A note on the identification of a Gulf Stream spin-off eddy from Eulerian data. *Geophys. Res. Lett.*, **7**, 549–552.

Richardson, W. S., W. J. Schmitz, Jr., and P. P. Niiler, 1969: The velocity structure of the Florida Current from the Straits of Florida to Cape Fear. *Deep-Sea Res.*, **16**(Suppl.), 225–231.

Schmitz, W. J., Jr., and P. P. Niiler, 1969: A note on the kinetic energy exchange between fluctuations and mean flow in the surface layer of the Florida current. *Tellus*, **21**, 814–819.

Webster, R., 1961a: A description of Gulf Stream meanders off Onslow Bay. *Deep-Sea Res.*, **9**, 130–143.

——, 1961b: The effect of meanders on the kinetic energy balance of the Gulf Stream. *Tellus*, **13**, 392–401.

White, J., 1952: The 1590 voyage and the search for the lost colony. *The Roanoke Voyages*, Vol. 2, D. Quinn, Ed., Hakluyt Society, London, 579–716 (see p. 608).